Macromolecules

pubs.acs.org/Macromolecules Article

Craze Extension Ratio of Semiflexible Polymer Glasses

Kai Nan and Robert S. Hoy*

Cite This: Macromolecules 2023, 56, 8369–8375 Read Online

ACCESS | Metrics & More | Article Recommendations | Supporting Information

ABSTRACT: Using molecular dynamics simulations, we show semiflexible bead–spring polymer glasses' craze extension ratio $\lambda_{craze} \gtrsim (N_e/\sqrt{C_\infty})^{1/2}$, where N_e is their entanglement length and C_∞ is their Flory characteristic ratio, over the entire range of chain stiffnesses for which their parent melts remain isotropic ($1 \leq N_e/C_\infty \lesssim 28$). Kramer's classic prediction $\lambda_{craze} = \sqrt{N_e/C_\infty}$ qualitatively captures trends for flexible chains with small C_∞, but quantitatively fails badly over the entire range of N_e/C_∞ studied here because it incorrectly treats Kuhn segments as rigid and inextensible. As a consequence, polymer glasses with N_e/C_∞ all the way down to the lower bound set by the onset of nematic order ($N_e/C_\infty = 1$) can exhibit a stable craze drawing and a ductile mechanical response.

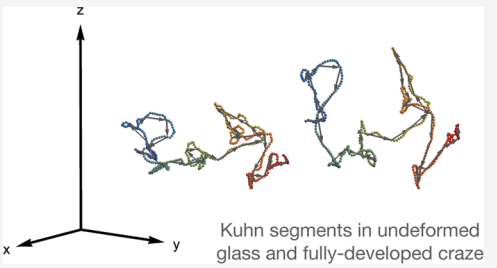

1. INTRODUCTION

Ductile glassy polymers' exceptional fracture toughness owes primarily to their ability to form mechanically stable crazes and shear bands. The geometrical structure of crazes in commodity-polymer glasses, which are composed of rather flexible chains whose entanglement length N_e is at least 4 times their Flory characteristic ratio C_∞,[1] was theoretically explained by Donald and Kramer over 40 years ago.[2,3] In their theory, the craze extension ratio λ_{craze}, which is experimentally defined as the ratio ρ_u/ρ_{fd} of the densities of undeformed glass and fully developed crazes (i.e., crazes away from the interfacial region),[3,4] is determined by the extent to which chains can stretch between cross-link-like entanglements without breaking. Entangled strands are treated as (N_e/C_∞)-link freely jointed chains that are Gaussian coils in the undeformed glass and perfectly straight in the fully developed craze. Since the links are treated as rigid rods of length l_K (the Kuhn length), the mean-squared end-end distances of the entangled strands in the undeformed glass and fully developed craze are $\langle R^2\rangle_u = (N_e/C_\infty)l_K^2$ and $\langle R^2\rangle_t = (N_e/C_\infty)^2 l_K^2$, respectively. The theory predicts that

$$\lambda_{craze} = \sqrt{\frac{\langle R^2\rangle_t}{\langle R^2\rangle_u}} = \sqrt{\frac{N_e}{C_\infty}} \tag{1}$$

A modified version of the same theoretical argument, which accounts for strands' projections along the directions parallel and perpendicular to the direction along which tensile stress is applied, predicts glasses' fracture stretch

$$\lambda_{frac} = \sqrt{\frac{3N_e}{C_\infty} - 2} \tag{2}$$

Remarkably, N_e values obtained from measurements of the melt plateau modulus ($G_N^0 = 4\rho k_B T/5N_e$) were found to successfully predict trends in λ_{craze} and λ_{frac} for a wide range of flexible polymer glasses (FPGs) in both experiments and simulations.[3,5] As a consequence, Kramer's theoretical picture has been widely accepted as correct for these systems for decades.[6,7]

In both real and simulated polymer melts, N_e/C_∞ is bounded from below by the onset of nematic order at $N_e/C_\infty \simeq 1$.[8−10] Kramer's theory predicts that glassy polymers will become brittle in this limit. Specifically, it predicts that systems with $N_e = C_\infty$ will have $\lambda_{frac} = \lambda_{craze} = 1$ and thus will be unable to form stable crazes or shear bands. This prediction casts doubt on the ability of semiflexible conjugated polymers (SCPs), which are currently attracting great interest owing to their potentially unique combination of electronic and mechanical properties,[9−16] to form ductile glasses. On the other hand, eqs 1 and 2 are based on three assumptions of questionable validity: (i) entangled strands in the undeformed glass can be accurately modeled as Gaussian coils; (ii) entangled strands act like chemical cross-links and pull completely taut prior to fracture; and (iii) Kuhn segments act like rigid links during sample deformation. None of these assumptions are very accurate for semiflexible polymer glasses (SPGs).

As a first step toward resolving this issue, we recently simulated crazing in a model SPG with $N_e = C_\infty$.[17] We showed that this system can stably craze-draw and in fact exhibits a mechanical response that is qualitatively the same as that of its

Received: August 11, 2023
Revised: September 20, 2023
Published: October 6, 2023

https://doi.org/10.1021/acs.macromol.3c01608
Macromolecules 2023, 56, 8369−8375

flexible counterparts. We explained this result in terms of the Kramer theory's failure to account for chain stretching at the Kuhn-segment scale [i.e., the failure of assumption (iii)]. Our model also treats entangled strands as (N_e/C_∞)-link freely jointed chains that are random coils in the undeformed glass and perfectly straight in the fully developed craze, but it assumes that the chain links are extensible and pull taut as the polymer is drawn into the craze. It postulates that—at least at the level of a mean-field scaling theory prediction—they can be captured by assuming that Kuhn segments stretch by a factor of $C_\infty^{1/4}$ as chains are drawn into craze fibrils.[1] As a consequence, it predicts that

$$\lambda_{craze} = \left(\frac{N_e}{\sqrt{C_\infty}}\right)^{1/2} \tag{3}$$

and

$$\lambda_{frac} = \left(3\frac{N_e}{\sqrt{C_\infty}} - 2\right)^{1/2} \tag{4}$$

These expressions quantitatively agreed with our simulation results for λ_{craze} and λ_{frac},[17] but have yet to be tested for systems with a wide range of N_e/C_∞. More fundamentally, the question of how formulas like eqs 1−4 can make accurate predictions even when all of the assumptions (i−iii) are inaccurate remains open. With the exception of our recent study,[17] previous experiments[2−4,18−21] and simulations[5,22−24] that measured λ_{craze} and λ_{frac} only examined FPGs with $N_e/C_\infty \gtrsim 4$. SCPs with $N_e \lesssim 2C_\infty$ are now available,[10] but so far, they have only been synthesized in small quantities, and their glassy-state mechanical properties have yet to be investigated. Thus, there is a great opportunity to obtain key insights into these systems' mechanics using coarse-grained computer simulations.

In this article, using molecular dynamics (MD) simulations of a standard coarse-grained model, we study crazing in polymer glasses spanning the entire range of chain stiffnesses for which their parent melts remain isotropic. We find that eq 3 quantitatively predicts λ_{craze} for SPGs (glasses with $N_e/C_\infty \lesssim 4$), provides a lower bound for λ_{craze} in FPGs (glasses with $N_e/C_\infty \gtrsim 4$), and outperforms eq 1 over the entire range of N_e/C_∞ studied here ($1 \leq N_e/C_\infty \lesssim 28$). We also find that eq 4 semiquantitatively predicts λ_{frac} for SPGs and provides an upper bound for λ_{frac} in FPGs. We demonstrate that the assumption[17] giving rise to the differences between eqs 3 and 4 and eqs 1 and 2—that Kuhn segments stretch by a factor $\sim C_\infty^{1/4}$ as they are drawn into the craze—is, in fact, correct for bead−spring SPGs. Finally, we explain why these quantitative discrepancies have not been noticed in previous work and show that the most essential novel result of ref 17 —that SPGs can be far more ductile than previously expected—is not specific to deformation protocols that produce strong triaxial tensile stresses and induce craze formation, but instead is robust against changing to drastically different deformation modes like uniaxial-stress tensile deformation and constant-volume simple shear.

2. MODELS AND METHODS

All MD simulations are performed using LAMMPS.[25] We employ the semiflexible, breakable-bond variant of the Kremer−Grest model.[26−28] Monomers have mass m and interact via the truncated and shifted Lennard−Jones potential $U_{LJ}(r) = 4\varepsilon[(a/r)^{12} - (a/r)^6 - (a/r_c)^{12} + (a/r_c)^6]$, where ε is the intermonomer binding energy, a is the monomer diameter, and $r_c = 2^{7/6}a$ is the cutoff radius. The Lennard−Jones time unit is $\tau = \sqrt{ma^2/\varepsilon}$, and the MD time step employed in this study is $\delta t = \tau/200$. Covalent bonds are modeled using a quartic potential commonly employed in studies of glassy-polymeric fracture[28]

$$U_{bond}(l) = k_q(l - R_b)^3(l - R_b - B_2) \tag{5}$$

As in ref 17, we set $B_2 = -0.4668a$ and $k_q = 4431\varepsilon/a^4$. The latter choice sets the ratio of the forces at which covalent and van der Waals bonds break to 50; this choice makes bond scission slightly easier than in many previous studies.[5,29] Variable chain stiffness is modeled using the standard potential $U_{ang}(\theta) = \kappa\varepsilon[1 - \cos(\theta)]$, where θ is the angle between consecutive covalent-backbone bond vectors and is zero for straight trimers.

Polymer melts composed of $N_{ch} = 250-1000$ linear chains of $N = 400-1600$ monomers were thoroughly equilibrated at $T = \varepsilon/k_B$ as described in ref 30. Numerical values of N_e/C_∞ for all systems are given in Table 1. The simulated systems spanned nearly the entire range of positive κ ($0.5 \leq \kappa \leq 5.5$) for which melts remain isotropic at this temperature,[27] and a range of N_e/C_∞ values ($1 \leq N_e/C_\infty \lesssim 28$) which is wider than the range spanned by real flexible and semiflexible polymer melts.[1,10] In contrast to the $\kappa \leq 2$ systems employed in most previous bead−spring crazing studies,[5,22−24] systems with $2.5 \leq \kappa \leq 5.5$ span the range $1 \leq N_e/C_\infty \leq 4$, i.e., the range of N_e/C_∞ values corresponding to SPGs.[10] All systems contained $N_{ch}N = 4 \times 10^5$ monomers and had $N \gtrsim 20N_e$, so finite-system-size and finite-N corrections to λ_{craze} and λ_{frac} should be minimal.[5]

Table 1. Values of N_e/C_∞ for the Systems Employed in This Study[a]

κ	N_e/C_∞	κ	N_e/C_∞
0.5	28	3.5	1.9
1.0	17	4.0	1.5
1.5	9.5	4.5	1.3
2.0	5.7	5.0	1.1
2.5	3.6	5.5	1.0
3.0	2.5		

[a] N_e and C_∞ were obtained as described in ref 31.

Here, we focus on crazing at a single temperature ($T = 0$) and deformation protocol (uniaxial-strain extension) that both favor brittle deformation.[5−7] After slowly cooling the equilibrated melts to $T = 0$ as described in ref, 29, we extended systems along their z-axis at a constant true strain rate $\dot{\epsilon} = 10^{-5}/\tau$ that is small enough to be near the quasistatic limit. Systems were deformed until they had extended well beyond fracture. Results for higher T will be discussed in an upcoming publication, and results for other deformation protocols are discussed in Appendix.

3. RESULTS

Figure 1 summarizes the mechanical and structural responses of selected systems to the applied deformation. Panel (a) shows the longitudinal stresses as a function of the true strain $\epsilon \equiv \ln(\lambda)$, where λ is the applied uniaxial stretch. All systems' initial elastic responses are followed by sharp yielding and massive strain softening, then by stress plateaus corresponding to stable craze drawing, then strain hardening, and finally fracture at stretches $\lambda_{frac}(\kappa)$ that we identify with the post-yield stress maxima.[2] Low-κ systems' strain softening is stronger and strain hardening is weaker than in previous comprehensive simulations of FPG crazing,[5,24] respectively because we prepared systems using a slower thermal quench than was employed in those studies and because our chains' backbone bonds break somewhat more easily. Critically, however, all

https://doi.org/10.1021/acs.macromol.3c01608
Macromolecules 2023, 56, 8369−8375

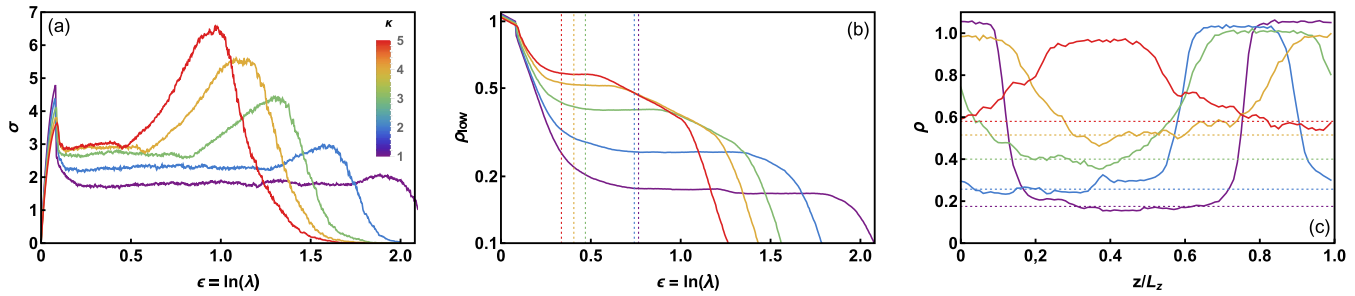

Figure 1. Stress–strain curves [panel (a)], average density of the lowest-ρ 25% transverse slice [panel (b)], and longitudinal density distributions at $\lambda = \lambda_{onset}(\kappa)$ [panel (c)] for bead–spring polymer glasses at $T = 0$. Vertical dotted lines in panel (b) indicate $\lambda = \lambda_{onset}(\kappa)$, while horizontal dotted lines in panel (c) indicate $\rho_{fd}(\kappa)$.

systems' stress–strain curves are qualitatively the same as those reported in refs. 5,24.

As mentioned above, experimental values of λ_{craze} are identified using the relation $\lambda_{craze} = \rho_u/\rho_{fd}$, where ρ_u and ρ_{fd} are, respectively, the densities of the undeformed glass and fully developed crazes.[2−4] Here, we mimic this procedure by dividing our systems into 100 slices along their z-axis and defining ρ_{low} as the average monomer number density of the least-dense 25% of these slices. As shown in panel (b), for all systems, $\rho_{low} \sim 1/\lambda$ in the initial elastic regime where systems deform homogeneously. Next, it drops sharply as crazes are nucleated when the systems yield.[32,33] Then it plateaus over a range of ϵ that closely corresponds to the stress plateau [panel (a)]. Finally, it drops again, slowly during strain hardening and rapidly upon fracture. We define $\lambda_{onset}(\kappa)$ as the stretches corresponding to the beginnings of the plateaus in ρ_{low}, i.e., as the macroscopic longitudinal stretches at the onset of stable craze drawing. Panel (c) shows systems' monomer number density profiles $\rho(z)$ at $\lambda = \lambda_{onset}(\kappa)$. All systems exhibit the coexisting high- and low-density regions typical of systems with mechanically stable crazes. We define $\rho_{fd}(\kappa)$ as the average densities of the latter regions, as indicated by the horizontal dotted lines. Note that this definition leads to estimates $\lambda_{craze}(\kappa) = \rho_u(\kappa)/\rho_{fd}(\kappa)$ that are slightly higher than[24] those obtained by identifying λ_{craze} with the onset of strain hardening as was done in ref. 5.

Figure 2 shows all systems' λ_{craze} and λ_{frac}, as a function of both κ [panel (a)] and N_e/C_∞ [panel (b)]. The measured $\lambda_{craze}(\kappa)$ values are within 10% of eq 3's prediction for all $\kappa \geq 3$, i.e., for all our model SPGs except the most flexible ($\kappa = 2.5$; see Table 1). For smaller-N_e/C_∞ glasses, eq 3 consistently underpredicts the measured λ_{craze}, but by no more than ∼20%. As we will discuss in more detail below, this underprediction may be associated with a failure of eq 3's assumptions that entangled strands start off as Gaussian coils and pull fully taut during crazing, that the strands orient independently of one another, that Kuhn segments stretch by a factor of $C_\infty^{1/4}$ as they are drawn into the craze, or with some combination of these factors. The measured $\lambda_{frac}(\kappa)$ values are within 10% of eq 4's prediction for all $\kappa \geq 1.5$, i.e., for all SPGs and also for all FPGs with $N_e/C_\infty < 10$. For larger-N_e/C_∞ glasses, eq 4 more substantially overpredicts the measured λ_{craze}, perhaps because it ignores cooperative chain scission events wherein scission of a weaker (or unusually highly stretched) entangled strand triggers further scission of the surrounding chains; see Section 4.

In contrast, eq 1 drastically underpredicts λ_{craze} for all systems, but since its predictions differ from those of eq 3 by a factor of only $C_\infty^{1/4}$, it correctly predicts the trends in λ_{craze} for small-C_∞ FPGs, partially explaining why it became so well accepted.[6,7] Equation 2 similarly underpredicts λ_{frac} for SPGs, but it overpredicts it for FPGs. While it does a rather poor job of capturing the variation of λ_{frac} with chain stiffness, its agreement with the measured values for $\kappa \leq 1$ is better than that of eq 4. Note that while multiplying the right-hand side of eq 1 by $\sqrt{3}$ (as was suggested in refs 3,24) makes its predictions more accurate, making the prediction $\lambda_{craze} = \sqrt{3N_e/C_\infty}$ seems to preclude developing a separate prediction for a larger λ_{frac} that could agree with the trends shown in Figure 2.

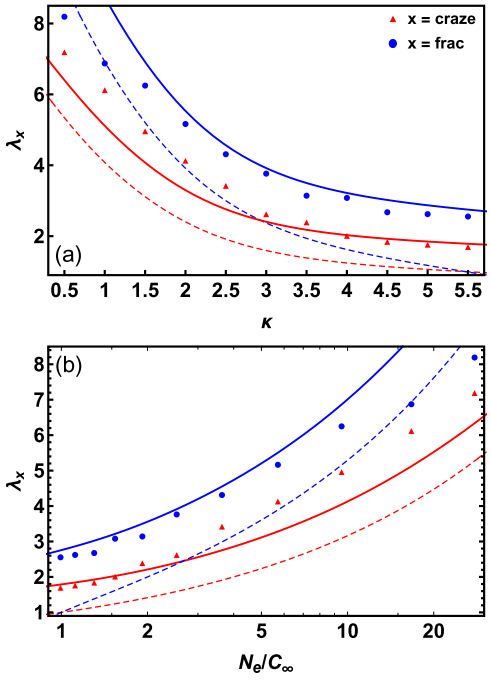

Figure 2. Measured vs predicted values of λ_{craze} and λ_{frac} for bead–spring polymer glasses at $T = 0$. Panel (a) shows results as a function of the chain stiffness parameter κ, while panel (b) shows the same results as a function of N_e/C_∞. Symbols show simulation results, solid curves show eqs 3 and 4, and dotted curves show eqs 1 and 2. Statistical errors in the simulation results (i.e., sample-to-sample variations of λ_{craze} and λ_{frac} for our employed $N_{ch}N$) are estimated to be less than 5%.

There is a simple explanation for why Kramer's classic expression for λ_{craze} fails even for FPGs. The original definition of the Kuhn length is[34]

https://doi.org/10.1021/acs.macromol.3c01608
Macromolecules 2023, 56, 8369−8375

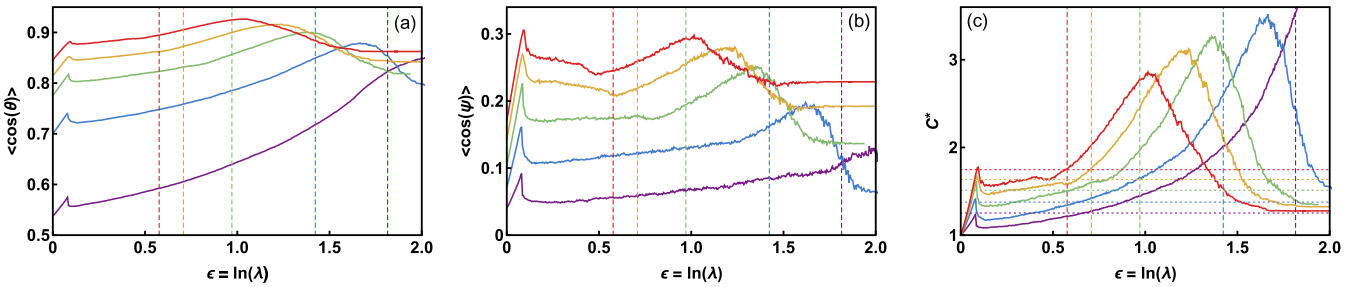

Figure 3. Effect of deformation on bead−spring polymer glasses' average bond and dihedral angles. Panel (c) shows the ratio $[C^*(\lambda)]$ of the strain-dependent C_{eff} values (eq 8) to their values in the undeformed glass. Vertical dashed and horizontal dotted lines, respectively, indicate $\lambda = \lambda_{craze}(\kappa)$ and $C^* = C_\infty^{1/4}(\kappa)$, where the C_∞ values are taken from the parent melts.[31] Averages are taken over all of the bond and dihedral angles in each system. Colors are the same as in Figure 1.

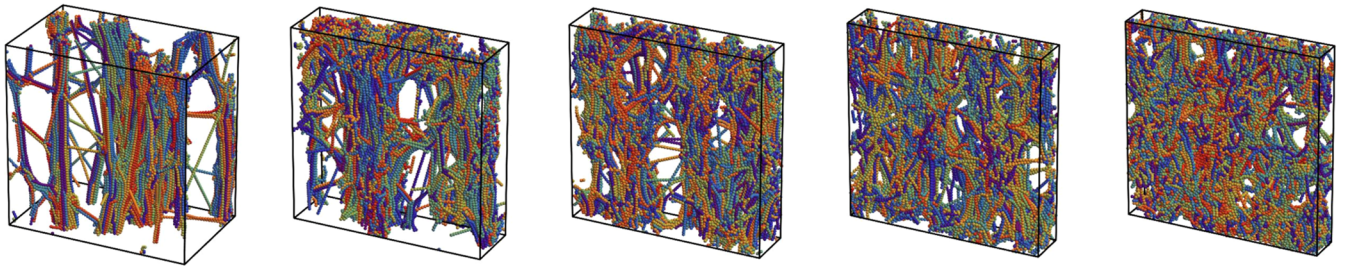

Figure 4. Snapshots of the craze structure in systems at $\lambda = \lambda_{craze}(\kappa)$. Images from left to right show results for κ = 1, 2, 3, 4, and 5. All images show regions of size $70a \times l_y \times 70a$, where the thickness l_y is chosen to make them all show the same number of monomers (30,000). Different colors indicate monomers belonging to different chains.

$$l_K = l_0\left(\frac{1+\langle\cos(\theta)\rangle}{1-\langle\cos(\theta)\rangle}\right)\left(\frac{1+\langle\cos(\psi)\rangle}{1-\langle\cos(\psi)\rangle}\right) \tag{6}$$

where θ and ψ are, respectively, the bond and dihedral angles formed by three and four consecutive monomers along chain backbones. Kramer's model (and indeed, all of the above discussion of quantities involving C_∞), however, defines the Kuhn length as

$$l_K = \frac{1+\langle\cos(\theta)\rangle}{1-\langle\cos(\theta)\rangle} l_0 \equiv C_\infty l_0 \tag{7}$$

Equation 7 is the definition more commonly employed in theories of polymer melt rheology and glassy polymer mechanics.[6,7,35] Since it treats C_∞ as fixed, it implicitly assumes both that $\langle\cos(\theta)\rangle$ remains constant and that $\langle\cos(\psi)\rangle = 0$ throughout the deformation process.

As shown in Figure 3, both of these assumptions fail badly for bead−spring glasses: $\langle\cos(\theta)\rangle$ and $\langle\cos(\psi)\rangle$ increase sharply in the elastic regime, and although they drop upon yielding, their values remain substantially higher than they were in the undeformed glass. As a consequence, the effective characteristic ratios

$$C_{eff} = \left(\frac{1+\langle\cos(\theta)\rangle}{1-\langle\cos(\theta)\rangle}\right)\left(\frac{1+\langle\cos(\psi)\rangle}{1-\langle\cos(\psi)\rangle}\right) \tag{8}$$

increase substantially as chains are drawn into craze fibrils. Panel (c) shows that in the limit $N_e/C_\infty \to 1$, the fractional increases in C_{eff} over the range $1 \le \lambda \le \lambda_{craze}$ are quantitatively consistent with Kuhn segments stretching by a factor $C_\infty^{1/4}$, as predicted by our model.[17] In this limit, the coexistence of crazed and unyielded regions at equal longitudinal stress (a criterion that must ultimately set the actual value of λ_{craze}[3,24]) appears to correspond to the coexistence of these regions at equal $C^*(\lambda_{yield}) = C^*(\lambda_{craze}) = C_\infty^{1/4}(\kappa)$. The assumption of constant C_{eff} should also fail in real polymer glasses, where it is known that tensile plastic deformation occurs largely through irreversible dihedral transitions that tend to increase $\langle\cos(\psi)\rangle$.[6]

Our observation that $C^*(\lambda_{craze}) > C_\infty^{1/4}$ for FPGs is consistent with eq 3's underprediction of these systems' λ_{craze} values. Strictly speaking, our model's treatment of Kuhn segments as being composed of $\sqrt{C_\infty}$ statistical segments, each of which contains $\sqrt{C_\infty}$ monomers, only makes physical sense for $C_\infty \gg 1$, and thus it must be expected to break down for FPGs with $C_\infty \sim 1$, e.g., for bead−spring glasses with $\kappa \lesssim 2.5$. Thus it is intriguing that all systems have $C^*(\lambda_{yield})$ values that are within less than 10% of their $C_\infty^{1/4}(\kappa)$.

To provide a better sense of how the results presented above connect to the craze microstructure, Figure 4 shows $\lambda = \lambda_{craze}(\kappa)$ snapshots of the same systems highlighted in Figure 1. All snapshots show orthorhombic regions of the same length ($70a$) along the longitudinal (z) direction and one transverse (x) direction; their lengths along the other transverse (y) direction are adjusted to make all snapshots show the same number of monomers. The leftmost panel (κ = 1) shows the characteristic FPG-craze-fibril structure, which was studied in great detail in refs 5,24. Chains in the primary fibrils are highly aligned along the z-axis, while the much smaller cross-tie fibrils appear to be randomly oriented. The rightmost three panels (κ = 3, 4, and 5) show that the SPG crazes' microstructure differs from the FPG-craze microstructure in two key respects: First, as expected from their lower λ_{craze} values, the chains in SPG craze fibrils are much less aligned along the longitudinal direction. Second, the distinction between primary and cross-tie fibrils, in terms of both their characteristic diameters and their characteristic orientations, is much less clear. Comparing Figures 2 and 4 suggests that eqs 3 and 4 accurately predict λ_{craze} and λ_{frac} for polymer glasses whose craze microstructure

https://doi.org/10.1021/acs.macromol.3c01608
Macromolecules 2023, 56, 8369−8375

resembles those shown in the rightmost three (but not the leftmost) snapshots. Note, however, that κ-dependent differences in bead−spring crazes' structure are strongly T-dependent;[5,17] this issue will be explored in more detail in an upcoming publication.

4. DISCUSSION AND CONCLUSIONS

In this paper, we supplied extensive simulation evidence that SPGs with N_e/C_∞ all the way down to the lower bound set by the onset of nematic order ($N_e/C_\infty = 1$) are capable of exhibiting stable craze drawing and a ductile mechanical response. We showed that accounting for Kuhn segments' ability to stretch during sample deformation yields an expression for the craze extension ratio λ_{craze} (eq 3) that outperforms Kramer's classic expression (eq 1) for polymer glasses spanning the entire range of chain stiffnesses for which their parent melts remain isotropic. As shown in Figure 2, the predictions of eq 3 are nearly quantitatively accurate for SPGs and provide a lower bound on λ_{craze} for FPGs that is well above eq 1's prediction.

Given the ubiquity of the widely accepted eqs 1 and 2, it is important to explain why the incorrect assumption leading to their failure was not noticed decades ago. One reason is the large uncertainties on both simulated and experimental values of λ_{craze}, N_e, and C_∞. Here, we showed that eq 1 underpredicts bead−spring FPGs' λ_{craze} by 25−45%. Reference 24 found that eq 1 undepredicted λ_{craze} for $\kappa = 0$, 0.75, and 1.5 by amounts similar to those reported here (i.e., 15−25%), but since results were obtained only for these three κ values and these discrepancies are comparable to the scatter of λ_{craze} values in the most comprehensive experimental studies performed to date,[2,3] they did not appear to require further investigation. Reference 5, a very careful study of the relation of craze structure to chain structure, examined the same range of κ as ref 24, but since this study used a less accurate method of estimating λ_{craze} (i.e., identifying it with the onset of strain hardening) and employed both flawed N_e-estimators[36] and parent melts that were poorly equilibrated, the systematic errors on its predicted and measured λ_{craze} were also comparable to the scatter of the experimental data.

Another reason the failure of eqs 1 and 2 was not noticed much earlier is that no previous studies of crazing examined a set of systems with closely spaced N_e/C_∞ values extending over a sufficiently wide range. Experiments did not demonstrate the qualitative failure of eq 1 for SPGs because (as mentioned above) polymers with $N_e/C_\infty < 4$ have been synthesized only recently[10,14] and their glassy-state mechanical properties remain largely unexplored. On the simulation side, since even the most comprehensive bead−spring studies of crazing to date[5,24] employed only a few $\kappa \leq 1.5$, no studies prior to the present one obtained a data set that could illustrate the breakdown of eqs 1 and 2 as we did in Figure 2.

Rudimentary chain-geometry-based predictions like eqs 1−4 necessarily miss much of the physics that controls craze structure. They ignore the fact that entangled strands are not Gaussian coils in undeformed glasses and are not perfectly straight in fully developed crazes. They ignore the fact that entangled stands cannot orient/stretch independently of their neighbors and that they are (apparently) constrained by their rheological tubes rather than by individual entanglements that act like chemical cross-links.[24] They ignore all considerations of mechanical force balance; λ_{craze} must in fact be determined by the requirement that unyielded and crazed regions coexist at equal longitudinal stress, and this coexistence occurs well before entangled strands pull taut.[3,24]

The ability of eqs 3 and 4 to accurately predict SPGs' λ_{craze} and λ_{frac} despite all of the above-mentioned oversimplifications likely results from a fortuitous cancellation of errors. For example, eq 4's faulty assumption that entangled strands pull fully taut before breaking should lead to an overestimation of λ_{frac}, but its faulty assumption that entanglements act like chemical cross-links should lead to an underestimation. The physical validity of expressions like eqs 3 and 4 should therefore be taken with more than a grain of salt. Nevertheless, since developing a microscopic theory of the craze structure that corrects all of the above-mentioned errors has proven to be an elusive goal, they remain useful for predicting the outcomes of simulations and, one may hope, future experiments on ductile SPGs. The extensive track record of bead−spring models in successfully explaining previously-poorly-understood aspects of glassy polymer mechanics[7] suggests that these expressions should predict the response of real SPGs, at least for simply structured (chemically homogeneous linear-polymeric) SPGs like the ones considered here.

Whether they will prove useful for predicting the mechanical response of suitably engineered SCPs is an open question. Solid SCPs that are sufficiently good conductors to be well-suited for electronics applications are usually quite brittle.[14,15] There are many potential reasons for the discrepancy between this experimental fact and the ductile mechanical responses reported above. One trivial reason is that the chains in many of the good-conducting SCP solids studied in the past have been weakly entangled (with a contour length that is not much larger than their persistence length) and hence unable to support stable craze drawing.[14] Another is that real SCPs could fail via shear banding rather than crazing, as expected for densely entangled polymer glasses.[6,18,19] This cannot be ruled out, but we show in the Appendix that the highly ductile response of the bead−spring SPGs considered in this paper is robust against changing the applied deformation protocol to uniaxial-stress extension or constant-volume simple shear.

Other potential reasons for the discrepancy are more directly related to our modeling approach. Employing much larger system sizes and/or much lower thermal quench rates might make Kremer−Grest bead−spring SPGs substantially more brittle,[37,38] but this will remain untestable for at least the next few years due to limited computer power. Semicrystalline bead−spring SPGs might be substantially more brittle than their amorphous counterparts; this hypothesis could be tested using currently available crystallizable coarse-grained models[3,41,42] Alternatively, the discrepancy might arise from various factors specific to SCP solids' local intrachain and interchain structures, e.g., their degree of regioregularity and side chain architecture.[14−16] These effects of such factors on the ability of SCPs to form ductile solids could potentially be tested using (very computationally expensive) simulations of recently developed finer-grained SCP models.[43,44]

APPENDIX. DEFORMATION-PROTOCOL INDEPENDENCE OF KREMER−GREST SPGS' DUCTILITY

In the main text, we focused on results for a single deformation protocol (uniaxial-strain extension) that, because it is highly dilatative and produces strongly triaxial tensile stresses, is guaranteed to produce either stable craze growth or brittle fracture.[3,6] Here, we demonstrate that the most essential result

https://doi.org/10.1021/acs.macromol.3c01608
Macromolecules 2023, 56, 8369−8375

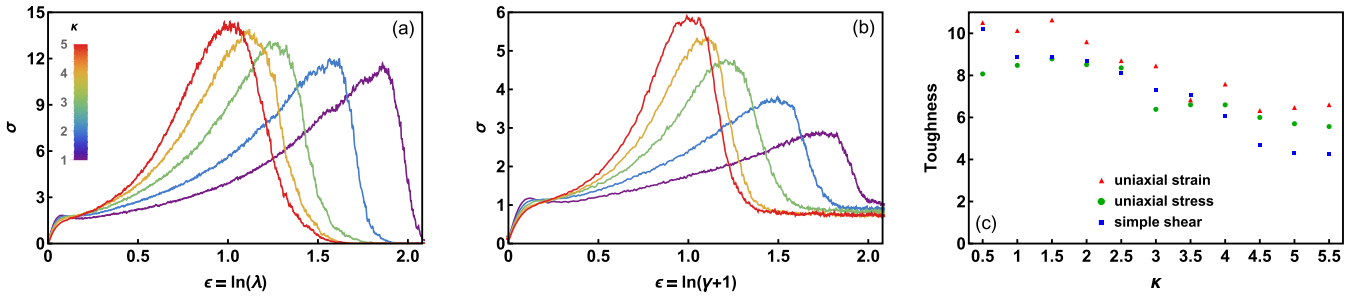

Figure 5. Mechanical response of SPGs under different deformation protocols. Panels (a, b), respectively, show the stress−strain curves for uniaxial-stress extension (extension along the z-direction with the transverse components of the stress maintained at zero) and constant-volume simple shear. In panel (b), σ is the shear stress and γ is the engineering shear strain. Panel (c) shows the tensile/shear toughnesses for all three protocols, here defined as the work per particle over the range $1 \le \lambda \le \lambda_{frac}$ or $0 \le \gamma \le \gamma_{frac}$; results for uniaxial strain correspond to those highlighted in Figures 1 and 2.

of both ref 17 and the present work—that SPGs can be far more ductile than previously expected—is robust against changing to a drastically different deformation mode.

Figure 5a,b, respectively, shows the stress−strain curves for uniaxial-stress tensile deformation and constant-volume simple shear,[25,33] for the same systems highlighted in Figure 1. These simulations employed the same applied strain rate used in the uniaxial-strain runs, i.e., $\dot{\epsilon} = 10^{-5}/\tau$. All trends are the same; as κ increases and N_e/C_∞ decreases, the degree of strain hardening and the fracture stress increase, and while the fracture strains decrease, systems remain ductile all the way to the $N_e/C_\infty \to 1$ nematic limit.

Figure 5(c) shows the toughnesses of these systems, i.e., the work per monomer performed by the applied deformation prior to fracture at $\lambda = \lambda_{frac}$ or $\gamma = \gamma_{frac}$. These are *not* the systems' fracture toughnesses, which are defined by the energy release rate or J integral rather than the area under stress−strain curves,[45] but are nonetheless a first-order measure of systems' ability to resist fracture. Results for all three deformation protocols show the same trends; toughness gradually decreases with increasing κ and decreasing N_e/C_∞, but it decreases by no more than a factor of ∼2.5 over the entire range of chain stiffnesses considered here. Thus, our results indicate that SPGs (or at least bead−spring SPGs with our employed system size and thermal quench rate) can be robustly tough.

■ ASSOCIATED CONTENT

Supporting Information

The Supporting Information is available free of charge at https://pubs.acs.org/doi/10.1021/acs.macromol.3c01608.

Potential improvements to eqs 3 and 4; validation of our mean-field scaling theory for Kuhn-segment scale stretching in SPGs; and an examination of the relative contributions of bond- and dihedral-angle opening to this stretching (PDF)

■ AUTHOR INFORMATION

Corresponding Author

Robert S. Hoy − *Department of Physics, University of South Florida, Tampa, Florida 33620, United States;* orcid.org/0000-0003-0283-8117; Email: rshoy@usf.edu

Author

Kai Nan − *Department of Physics, University of South Florida, Tampa, Florida 33620, United States*

Complete contact information is available at: https://pubs.acs.org/10.1021/acs.macromol.3c01608

Notes

The authors declare no competing financial interest.

■ ACKNOWLEDGMENTS

This material is based upon work supported by the National Science Foundation under Grant No. DMR-2026271.

■ ADDITIONAL NOTES

[1]Kuhn segments are able to stretch by this factor because they are composed of $\sqrt{C_\infty}$ statistical segments, each of which contains $\sqrt{C_\infty}$ monomers. Note that while experimental studies often define N_e as the number of statistical segments per entangled strand[1] rather than the number of monomers per entangled strand as we have done here, this alternative definition does not affect the above arguments; it reduces the N_e in eqs 1−4 by a factor of $\sqrt{C_\infty}$ and then sets $C_\infty = 1$.

[2]In other words, λ_{frac} is the stretch at which the longitudinal stress σ_{zz} has either its global or its post-yield maximum.

[3]Since stress tends to concentrate at (and cracks to propagate along) the boundaries between crystalline and amorphous regions,[39] and maximal stress concentrations scale approximately as $\sqrt{L}$,[40] making these tests conclusive might require simulating very large systems.

■ REFERENCES

(1) *Physical Properties of Polymers Handbook*, 2nd ed.; Mark, J. E., Ed.; Springer, 2007.

(2) Donald, A. M.; Kramer, E. J. Effect of Molecular Entanglements on Craze Microstructure in Glassy Polymers. *J. Polym. Sci., Polym. Phys. Ed.* **1982**, *20*, 899−909.

(3) Kramer, E. J. Microscopic and Molecular Fundamentals of Crazing. In *Advances in Polymer Science*; Springer, 1983; Vol. *52*, pp 1−56.

(4) Lauterwasser, B. D.; Kramer, E. J. Microscopic mechanisms and mechanics of craze growth and fracture. *Philos. Mag. A* **1979**, *39*, 469−495.

(5) Rottler, J.; Robbins, M. O. Growth, microstructure, and failure of crazes in glassy polymers. *Phys. Rev. E* **2003**, *68*, No. 011801.

(6) Haward, R. N.; Young, R. J. *The Physics of Glassy Polymers*; Chapman & Hall: London, 1997.

(7) *Polymer Glasses*; Roth, C. B., Ed.; CRC Press: Boca Raton, 2016.

(8) Hoy, R. S.; Kröger, M. Unified Analytic Expressions for the Entanglement Length, Tube Diameter, and Plateau Modulus of Polymer Melts. *Phys. Rev. Lett.* **2020**, *124*, No. 147801.

(9) Xie, R.; Aplan, M. P.; Caggiano, N. J.; Weisen, A. R.; Su, T.; Müller, C.; Segad, M.; Colby, R. H.; Gomez, E. D. Local Chain Alignment via Nematic Ordering Reduces Chain Entanglement in Conjugated Polymers. *Macromolecules* **2018**, *51*, No. 10271.
(10) Fenton, A. M.; Xie, R.; Aplan, M. P.; Lee, Y.; Gill, M. G.; Fair, R.; Kempe, F.; Sommer, M.; Snyder, C. R.; Gomez, E. D.; Colby, R. H. Predicting the plateau modulus from molecular parameters of conjugated polymers. *ACS Cent. Sci.* **2022**, *8*, 268−274.
(11) Rivnay, J.; Owens, R. M.; Malliaras, G. G. The Rise of Organic Bioelectronics. *Chem. Mater.* **2014**, *26*, 679−685.
(12) Liao, C.; Zhang, M.; Yao, M. Y.; Hua, T.; Li, L.; Li, L.; Yan, F. Flexible Organic Electronics in Biology: Materials and Devices. *Adv. Mater.* **2015**, *27*, 7493−7527.
(13) Xie, R.; Lee, Y.; Aplan, M. P.; Caggiano, N. J.; Müller, C.; Colby, R. H.; Gomez, E. D. Glass transition temperature of conjugated polymers by oscillatory shear rheometry. *Macromolecules* **2017**, *50*, 5146−5154.
(14) Xie, R.; Colby, R. H.; Gomez, E. D. Connecting the Mechanical and Conductive Properties of Conjugated Polymers. *Adv. Elect. Mater.* **2018**, *4*, No. 1700356.
(15) Ashizawa, M.; Zheng, Y.; Tran, H.; Bao, Z. Intrinsically stretchable conjugated polymer semiconductors in field effect transistors. *Prog. Polym. Sci.* **2020**, *100*, No. 101181.
(16) Son, S. Y.; Kim, J.-H.; Song, E.; Choi, K.; Lee, J.; Cho, K.; Kim, T.-S.; Park, T. Exploiting π-π Stacking for Stretchable Semiconducting Polymers. *Macromolecules* **2018**, *51*, 2572−2579.
(17) Dietz, J. D.; Nan, K.; Hoy, R. S. Unexpected Ductility in Semiflexible Polymer Glasses with Entanglement Length Equal to their Kuhn Length. *Phys. Rev. Lett.* **2022**, *129*, No. 127801.
(18) Donald, A. M.; Kramer, E. J. The competition between shear deformation and crazing in glassy polymers. *J. Mater. Sci.* **1982**, *17*, 1871−1879.
(19) Henkee, C. S.; Kramer, E. J. Crazing and Shear Deformation in Crosslinked Polystyrene. *J. Polym. Sci., Polym. Phys. Ed.* **1984**, *22*, 721−737.
(20) Berger, L. L.; Kramer, E. J. The effect of temperature on the transition from crazing to shear deformation in crosslinked polystyrene. *J. Mater. Sci.* **1988**, *23*, 3536−3543.
(21) Kramer, E. J.; Berger, L. L.Fundamental Processes of Craze Growth and Fracture. In *Advance Polymer Science* 1990; Vol. *91*, pp 1−68.
(22) Baljon, A. R. C.; Robbins, M. O. Simulations of Crazing in Polymer Glasses: Effect of Chain Length and Surface Tension. *Macromolecules* **2001**, *34*, 4200−4209.
(23) Rottler, J.; Barsky, S.; Robbins, M. O. Cracks and Crazes: On calculating the macroscopic fracture energy of glassy polymers from molecular simulations. *Phys. Rev. Lett.* **2002**, *89*, No. 148304.
(24) Ge, T.; Tzoumanekas, C.; Anogiannakis, S. D.; Hoy, R. S.; Robbins, M. O. Entanglements in Glassy Polymer Crazing: Cross-Links or Tubes? *Macromolecules* **2017**, *50*, 459−471.
(25) Thompson, A. P.; Aktulga, H. M.; Berger, R.; Bolintineanu, D. S.; Brown, W. M.; Crozier, P. S.; i'nt Veld, P. J.; Kohlmeyer, A.; Moore, S. G.; Nguyen, T. D.; Shan, R.; Stevens, M. J.; Tranchida, J.; Trott, C.; Plimpton, S. J. LAMMPS-a flexible simulation tool for particle-based materials modeling at the atomic, meso, and continuum scales. *Comput. Phys. Commun.* **2022**, *271*, No. 108171.
(26) Kremer, K.; Grest, G. S. Dynamics of Entangled Linear Polymer Melts: A Molecular-Dynamics Simulation. *J. Chem. Phys.* **1990**, *92*, 5057−5086.
(27) Faller, R.; Kolb, A.; Müller-Plathe, F. Local chain ordering in amorphous polymer melts: influence of chain stiffness. *Phys. Chem. Chem. Phys.* **1999**, *1*, 2071−2076.
(28) Stevens, M. J. Interfacial Fracture between Highly Cross-Linked Polymer Networks and a Solid Surface: Effect of Interfacial Bond Density. *Macromolecules* **2001**, *34*, 2710−2718.
(29) Nguyen, H. T.; Hoy, R. S. Effect of the ratio l_K/p on glassy-polymeric shear deformation mechanisms. *Macromolecules* **2018**, *51*, 4370−4380.
(30) Dietz, J. D.; Hoy, R. S. Facile equilibration of well-entangled semiflexible bead-spring polymer melts. *J. Chem. Phys.* **2022**, *156*, No. 014103.
(31) Dietz, J. D.; Kröger, M.; Hoy, R. S. Validation and refinement of unified analytic model for flexible and semiflexible polymer melt entanglement. *Macromolecules* **2022**, *55*, 3613−3626.
(32) Argon, A. S.; Hannoosh, J. G. Initiation of crazes in polystyrene. *Philos. Mag.* **1977**, *36*, 1195−1216.
(33) Rottler, J.; Robbins, M. O. Shear yielding of amorphous polymer glasses: effect of temperature and strain rate. *Phys. Rev. E* **2003**, *68*, No. 011507.
(34) Flory, P. J. *Principles of Polymer Chemistry*; Cornell University Press: Ithaca, NY, 1953.
(35) Doi, M.; Edwards, S. F. *The Theory of Polymer Dynamics*; Oxford: Oxford, 1988.
(36) Hoy, R. S.; Foteinopoulou, K.; Kröger, M. Topological analysis of polymeric melts: Chain-length effects and fast-converging estimators for entanglement length. *Phys. Rev. E* **2009**, *80*, No. 031803.
(37) Zhang, Z.; Ispas, S.; Kob, W. The critical role of the interaction potential and simulation protocol for the structural and mechanical properties of sodosilicate glasses. *J. Non-Cryst. Solids* **2020**, *532*, No. 119895.
(38) Ozawa, M.; Berthier, L.; Biroli, G.; Rosso, A.; Tarjus, G. Random critical point separates brittle and ductile yielding transitions in amorphous materials. *Proc. Natl. Acad. Sci. U.S.A.* **2018**, *115*, 6656−6661.
(39) Schultz, J. M. Microstructural Aspects of Failure in Semicrystalline Polymers. *Polym. Eng. Sci.* **1984**, *24*, 770−785.
(40) Xu, R. X.; Thompson, J. C.; Topper, T. H. Practical stress expressions for stress concentration regions. *Fatigue Fract. Eng. Mater. Struct.* **1995**, *18*, 885−895.
(41) Nguyen, H. T.; Smith, T. B.; Hoy, R. S.; Karayiannis, N. C. Effect of chain stiffness on the competition between crystallization and glass- formation in model unentangled polymers. *J. Chem. Phys.* **2015**, *143*, No. 144901.
(42) Morthomas, J.; Fusco, C.; Zhai, Z. Q.; Lame, O.; Perez, M. Crystallization of finite-extensible nonlinear elastic Lennard-Jones coarse-grained polymers. *Phys. Rev. E* **2017**, *96*, No. 052502.
(43) Zhang, W.; Bombile, J. H.; Weisen, A. R.; Xie, R.; Colby, R. H.; Janik, M. J.; Milner, S. T.; Gomez, E. D. Thermal Fluctuations Lead to Cumulative Disorder and Enhance Charge Transport in Conjugated Polymers. *Macromol. Rapid Commun.* **2019**, *40*, No. 1900134.
(44) Cohen, A. E.; Jackson, N. E.; de Pablo, J. J. Anisotropic Coarse-Grained Model for Conjugated Polymers: Investigations into Solution Morphologies. *Macromolecules* **2021**, *54*, 3780−3789.
(45) Anderson, T. L. *Fracture Mechanics: Fundamentals and Applications*, 4th ed.; CRC Press: Boca Raton, 2017.

https://doi.org/10.1021/acs.macromol.3c01608
Macromolecules 2023, 56, 8369−8375